Journal of Colloid and Interface Science 377 (2012) 207–212

Contents lists available at SciVerse ScienceDirect

Journal of Colloid and Interface Science

www.elsevier.com/locate/jcis

Auto-stratification in drying colloidal dispersions: A diffusive model

R.E. Trueman [a], E. Lago Domingues [b], S.N. Emmett [b], M.W. Murray [b], A.F. Routh [a,*]

[a] Department of Chemical Engineering and Biotechnology, University of Cambridge, Pembroke Street, Cambridge CB2 3RA, UK
[b] AkzoNobel, Wexham Road, Slough SL2 5DS, UK

ARTICLE INFO

Article history:
Received 15 February 2012
Accepted 15 March 2012
Available online 28 March 2012

Keywords:
Stratification
Diffusion
Colloidal hydrodynamics

ABSTRACT

The mechanism by which the particles in a drying film come into close packing during solvent evaporation has an important role to play in the final film morphology. During drying the particles can develop non-uniform concentrations across the vertical height of the film, depending on their diffusion rate. By applying the principles of classical diffusion mechanics to a hard sphere system, a theory for this novel method of stratification during drying of a two component film has been derived. The model is dependent on the particle Peclet numbers and when one is above unity and the other below, maximum stratification is observed.

1. Introduction

Stratification of particulate material is a phenomenon observed within many disciplines. One of the most well known examples is the 'Brazil Nut Effect', in which large particles rise to the top of a container of mixed size particles when agitated [1,2]. Larger soil particles have also been shown to vertically segregate to the top of a sample which has a vertically rising freezing front [3]. On the colloidal scale, particle transport processes can be dominated by sedimentation, diffusion and convection [4–7].

Latex film formation occurs through the process of solvent evaporation from a cast latex dispersion [8,9], resulting in the particles becoming closely packed. This process finishes with deformation and coalescence of the particles. Industrially these films typically contain many different components to impart their individual properties on the final dried product. During drying the films are not always vertically homogenous. It has been seen that some particles will preferentially migrate to the surface/air interface or the substrate [10]. Surfactant mobility to the surface/air interface has also been observed [11,12], along with movement of dissolved salts through pores in the film structure [13].

It is often desired that a composite film dries with a uniform vertical distribution of components. Grillet et al. [4] describes films formed from soft latex and hard silica particles, with the intention being to utilise the strength of the silica and the film forming ability of the latex. However, in one particular scenario the silica sedimented out, so that the film was silica rich near the substrate and latex rich near the surface/air interface, which was undesired. In certain situations, however, this type of structure can be advantageous, for example to create multi-layered coatings through one application step. Key applications for this kind of technology could be placing active components at the film/air interface, or a hard protective surface on top of a softer coating. A further potential use is demonstrated by Sun et al. who created a transparent, conductive coating by blending a film forming latex with a conducting polymer and ensuring the formation of a conducting network [14].

During the initial solvent evaporation step of film formation the particle volume fraction increases until close packing is reached. The formation of skin on the surface has been often observed [15–17]. This phenomena occurs as the particles collected by the descending top surface are unable to diffuse away into the bulk. This behaviour can be described by the Peclet number, which is the ratio of the evaporation rate against the diffusion rate, represented mathematically as

$$Pe_1 = \frac{6\pi\eta R_1 \dot{E} H}{kT}, \tag{1}$$

where R_1 is the particle radius, η the solvent viscosity, $\dot{E}$ the evaporation rate, H the initial film height and kT thermal energy. The subscript is used, throughout this paper, to refer to each particle type and type one always relates to the smaller particles in the film.

An increase in particle concentration at the film/air interface has been observed using NMR techniques [16,18,19] and modelled by Routh and Zimmerman [7]. At large Peclet numbers the diffusion is not sufficient to equilibrate the concentration gradient set up by the evaporation, so skin formation occurs (Fig. 1). At low Peclet numbers the particles are able to diffuse away from the surface into the bulk of the film (Fig. 2).

Consider a film cast from a dispersion containing two types of particle. If one of the particles has a high Peclet number and

* Corresponding author.
E-mail address: afr10@cam.ac.uk (A.F. Routh).

0021-9797/$ - see front matter © 2012 Elsevier Inc. All rights reserved.
http://dx.doi.org/10.1016/j.jcis.2012.03.045

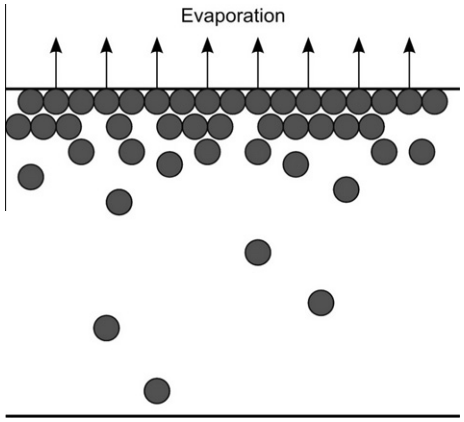

Fig. 1. Schematic of high Peclet number particle distribution within a drying film.

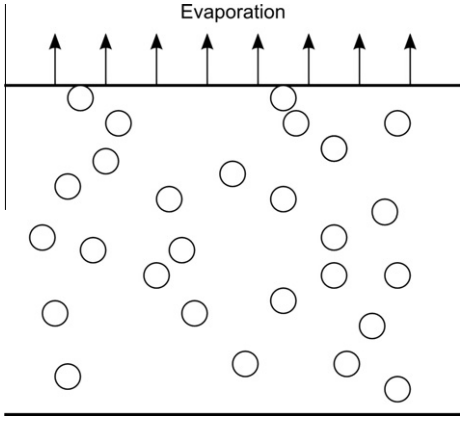

Fig. 2. Schematic of low Peclet number particle distribution within a drying film.

conversely the other has a low Peclet number then a self stratifying system will be set up, as seen in Fig. 3. The transition point between diffusion or evaporation being the dominant force is around a Peclet number of unity. Therefore, ideally the Peclet numbers of the two components should lie either side of this value. Assuming Stokes–Einstein diffusion, one method of changing the Peclet numbers of two components within a single film is to alter the particle radius. The larger particles will have a higher Peclet number, and so will be trapped at the evaporating top surface. It has been shown experimentally by Nikiforow et al. [20] that changing the charge on the particles so that one component has a charged surface, whereas the other does not, can also produce stratification based on differing diffusion rates. Studies of non-uniform particle

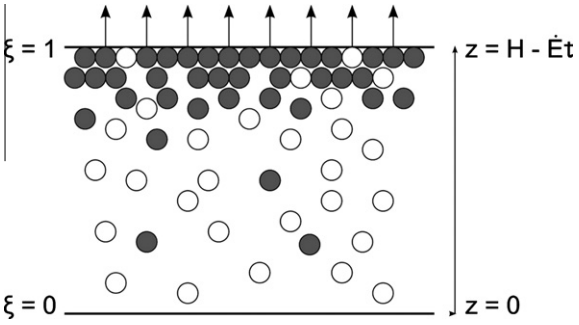

Fig. 3. Schematic of particle distribution within a drying film comprised of two components, the Peclet numbers of each lying either side of unity.

distributions have been carried out by Francis et al. using a large disparity in size [21,22] as well as using a free polymer to change particle diffusion along with colloidal stability [23]. A novel example of segregation is given by Harris et al. [24,25]. By drying films under a mask a horizontal flow is established to bring solvent into the evaporating regions. This flow carries particles and so allows for a horizontal as well as vertical segregation.

This paper develops a model for stratification of particles in bi-disperse particle mixtures. The model is based on classical diffusion and predicts that larger, slower moving, particles will preferentially accumulate at the air/water interface. A second paper [26] reports on experimental investigations into drying of particle mixtures. This work generally conforms with the diffusional model although it also demonstrates the inherent difficulty of obtaining completely stagnant, colloidally stable bi-disperse mixtures. Finally a third paper [27] demonstrates the importance of particle interactions in determining the degree of stratification.

2. Derivation of governing conservation equations for a two component film

For clarity this section merely contains the barest outline of the derivation and discusses the necessary assumptions. A full derivation can be found in the Supplementary information. For a film of fluid containing two types of particle of differing radius, the conservation equation for particles of type one is

$$\frac{\partial \phi_1}{\partial t} + \nabla \cdot \phi_1 \mathbf{U}_1 = 0, \tag{2}$$

where ϕ_1 is the volume fraction of component one and $\mathbf{U}_1$ is the volume average velocity, which in a static, drying film can be expressed as

$$\mathbf{U}_1 = -\frac{K(\phi_1, \phi_2)}{6\pi\eta R_1} \nabla \mu_1, \tag{3}$$

where μ_1 is the chemical potential of component one and $K(\phi_1, \phi_2)$ is the sedimentation coefficient, which is the ratio between the settling velocity at the local particle volume fraction and the Stokes settling velocity. The sedimentation coefficient accounts for the effect of particle crowding and the reduced diffusion coefficient in concentrated dispersions. It is possible to introduce a diffusion coefficient tensor, making the flux of component 1 also dependent on the gradient in the chemical potential of component 2. i.e. $j_1 = -D_{11}\nabla\mu_1 - D_{12}\nabla\mu_2$ [28]. We however prefer to ignore the off diagonal terms in the diffusion tensor. The basis for doing this, as discussed by Cussler [29], is that the magnitude of these terms are typically small. The final expression we derive (Eq. (7)) contains gradients in both component volume fractions, due to the coupling through the chemical potentials. This means that inclusion of a flux dependence on $\nabla\mu_2$ will alter the final conservation expressions slightly, but their functional form stays the same and any error is small.

To determine the chemical potential in a three component system the change in Gibbs energy upon addition of a single additional particle of a particular type must be considered. This derivation can be found in Section 3 of the Supplementary information and it demonstrates that the chemical potential of component 1 in a two component film is

$$\mu_1 = \mu_{P1} - \frac{1-\phi_1-\phi_2}{1-\phi_1}\frac{\frac{4}{3}\pi R_1^3}{v_s}\mu_s - \frac{\phi_2}{1-\phi_1}\left(\frac{R_1}{R_2}\right)^3 \mu_{P2}, \tag{4}$$

where μ_{P1} is the chemical potential of particles of type 1, v_s is the volume of one molecule of solvent. The Gibbs–Duhem relates the three chemical potentials in the system,

$$n_{P_1}\frac{\partial \mu_{P1}}{\partial \hat{z}} + n_{P_2}\frac{\partial \mu_{P2}}{\partial \hat{z}} + n_s\frac{\partial \mu_s}{\partial \hat{z}} = 0, \tag{5}$$

where n_{P_1} and n_{P_2} are the number densities of particles of components 1 and 2 respectively, and n_s is the number density of solvent molecules. The chemical potential of the solvent, μ_s, is related to the osmotic pressure as

$$\Pi = -\frac{\mu_s - \mu_s^0}{v_s} = \left(\frac{\phi_1}{\frac{4}{3}\pi R_1^3} + \frac{\phi_2}{\frac{4}{3}\pi R_2^3}\right) kTZ(\phi_1, \phi_2), \tag{6}$$

where μ_s^0 is the solvent reference potential and $Z(\phi_1, \phi_2)$ is the compressibility, which accounts for the non-ideality of the osmotic pressure at high volume fractions.

We solve the simplest problem possible, which is a film of initial thickness, H, evaporating at a constant rate $\dot{E}$. In this one-dimensional problem we scale vertical distances on the initial film thickness ($\hat{z} = z/H$) and time with the evaporation time ($\hat{t} = t/(H/\dot{E})$). For a film decreasing in height the position of the top boundary is time dependent. This can create numerical difficulties so it is easier to create a static spatial domain by defining $\xi = \frac{\hat{z}}{1-\hat{t}}$. The transformed variable for time is $\tau = \hat{t}$. Combining the above equations and noting that the particle transport is overwhelmingly driven by the divergence in the compressibility as close packing is reached, the conservation equation for species one is

which considers only the entropic contribution of each component to the chemical potential. In general the ratio of chemical potentials will be set by the surface chemistry as well as local concentration, so it is potentially controllable. Here we take the simplest possible case which is just the entropic terms. The full expression for the chemical potentials of particles of each component, which also contain enthalpic terms, has been shown by Lebowitz and Rowlinson [30].

The other expressions which must be defined in order to solve the system are the sedimentation coefficient and the compressibility. The sedimentation coefficient, $K(\phi)$ for the one component system solved by Routh and Zimmerman [7] was taken as $K(\phi) = (1-\phi)^{6.55}$ [31]. For the two component case the functional form was assumed to remain the same, so that $K(\phi_1, \phi_2) = (1-\phi_1-\phi_2)^{6.55}$. The compressibility of the dispersion for the one component system, $Z(\phi) = 1/(\phi_m - \phi)$ [31], is such that it diverges once the particles reach close packing. For the two component system this was taken as $Z(\phi_1, \phi_2) = \phi_m/(\phi_m - \phi_1 - \phi_2)$. This expression ensures divergence at close packing, yet equals unity in the dilute limit. Both of the expressions $K(\phi_1, \phi_2)$ and $Z(\phi_1, \phi_2)$ are in principle measurable experimentally.

$$\frac{\partial \phi_1}{\partial \tau} + \frac{\xi}{1-\tau}\frac{\partial \phi_1}{\partial \xi} = \frac{1}{Pe_1(1-\tau)^2} \times \frac{\partial}{\partial \xi}\left[\left[\frac{K(\phi_1,\phi_2)\phi_1\left[\phi_1(1-\phi_1)\frac{\partial \mu_{P1}/\partial \xi}{\partial \mu_{P2}/\partial \xi} - \phi_1\phi_2\left(\left(\frac{Pe_1}{Pe_2}\right)^3 + \frac{\partial \mu_{P1}/\partial \xi}{\partial \mu_{P2}/\partial \xi}\right) + \phi_2(1-\phi_2)\left(\frac{Pe_1}{Pe_2}\right)^3\right]}{(1-\phi_1)\left(\phi_1^2\frac{\partial \mu_{P1}/\partial \xi}{\partial \mu_{P2}/\partial \xi} + 2\phi_1\phi_2\left(\frac{Pe_1}{Pe_2}\right)^3 + \phi_2^2\left(\frac{Pe_1}{Pe_2}\right)^6\frac{\partial \mu_{P2}/\partial \xi}{\partial \mu_{P1}/\partial \xi}\right)}\right]\frac{\partial}{\partial \xi}\left[\left(\phi_1 + \left(\frac{Pe_1}{Pe_2}\right)^3\phi_2\right)Z(\phi_1,\phi_2)\right]\right]. \tag{7}$$

For component two, the conservation equation is

$$\frac{\partial \phi_2}{\partial \tau} + \frac{\xi}{1-\tau}\frac{\partial \phi_2}{\partial \xi} = \frac{1}{Pe_2(1-\tau)^2} \times \frac{\partial}{\partial \xi}\left[\left[\frac{K(\phi_1,\phi_2)\phi_2\left[\phi_2(1-\phi_2)\frac{\partial \mu_{P2}/\partial \xi}{\partial \mu_{P1}/\partial \xi} - \phi_2\phi_1\left(\left(\frac{Pe_2}{Pe_1}\right)^3 + \frac{\partial \mu_{P2}/\partial \xi}{\partial \mu_{P1}/\partial \xi}\right) + \phi_1(1-\phi_1)\left(\frac{Pe_2}{Pe_1}\right)^3\right]}{(1-\phi_2)\left(\phi_2^2\frac{\partial \mu_{P2}/\partial \xi}{\partial \mu_{P1}/\partial \xi} + 2\phi_2\phi_1\left(\frac{Pe_2}{Pe_1}\right)^3 + \phi_1^2\left(\frac{Pe_2}{Pe_1}\right)^6\frac{\partial \mu_{P1}/\partial \xi}{\partial \mu_{P2}/\partial \xi}\right)}\right]\frac{\partial}{\partial \xi}\left[\left(\phi_2 + \left(\frac{Pe_2}{Pe_1}\right)^3\phi_1\right)Z(\phi_1,\phi_2)\right]\right]. \tag{8}$$

The boundary conditions are no flux of material through the solid bottom substrate or through the moving top boundary. Explicit forms for the boundary conditions are given in the Supplemental information.

3. Functional form of parameters

The assumptions made in derivation of Eqs. (7) and (8) are that there is no bulk flow and that gravity is negligible. In addition the dispersions are taken to be colloidally stable. To provide solutions it is necessary to assume functional forms for the various parameters and to introduce a numerical scheme. This system of coupled PDEs was solved using an explicit forward in time, centred in space (FTCS) differencing scheme, which was coded in MATLAB. To close the set of equations, the ratio of the chemical potential gradients of the two components was represented as

$$\frac{\partial \mu_{P1}/\partial \xi}{\partial \mu_{P2}/\partial \xi} = \frac{\phi_2}{\phi_1}\frac{\partial \phi_1/\partial \xi}{\partial \phi_2/\partial \xi}, \tag{9}$$

4. Results and discussion

In order to evaluate the effect of changing conditions on the drying of films using this model, there are a few key parameters which can be altered. The first of these variables is the ratio of sizes between the two components, which is represented by Pe_1/Pe_2. The geometric mean Peclet number, $\sqrt{Pe_1Pe_2}$, is the other key variable. For a given Peclet ratio, if $\sqrt{Pe_1Pe_2} \ll 1$ with $Pe_1 < 1$ and $Pe_2 < 1$, then diffusion will be dominant for both components. If $\sqrt{Pe_1Pe_2} \gg 1$ with $Pe_1 > 1$ and $Pe_2 > 1$, then evaporation will be dominant and both components will be trapped at the top surface. When $\sqrt{Pe_1Pe_2} = 1$ then one of the components will be dominated by diffusion and the other by evaporation. A further variable to change is the ratio between the initial concentrations of each component. The final variable which can be altered is the total initial volume fraction.

Figs. 4–6 show examples of the evolution of volume fraction profiles over time. The horizontal axes show the position in space of the film, with $z/H = 0$ being the film/substrate interface and $z/H = 1$ being the film/air interface, at the start of the drying process.

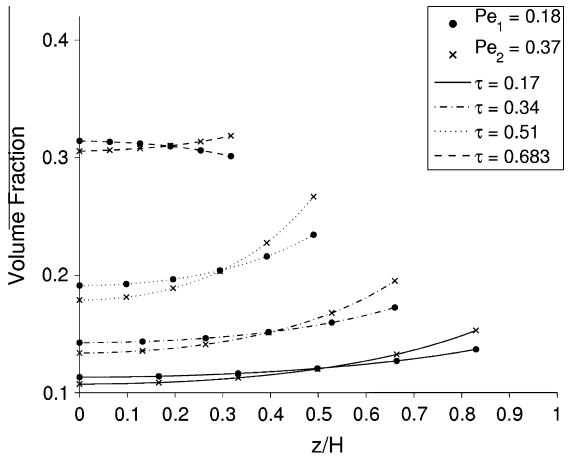

Fig. 4. Graph showing the evolution of volume fraction profiles during drying, both $Pe < 1$.

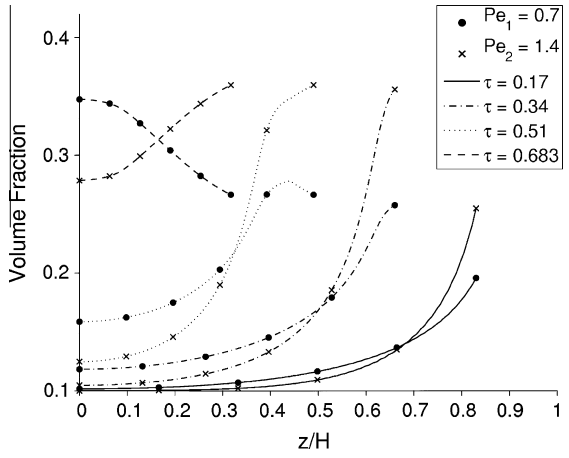

Fig. 5. Graph showing the evolution of volume fraction profiles during drying, $Pe_1 < 1$, $Pe_2 > 1$.

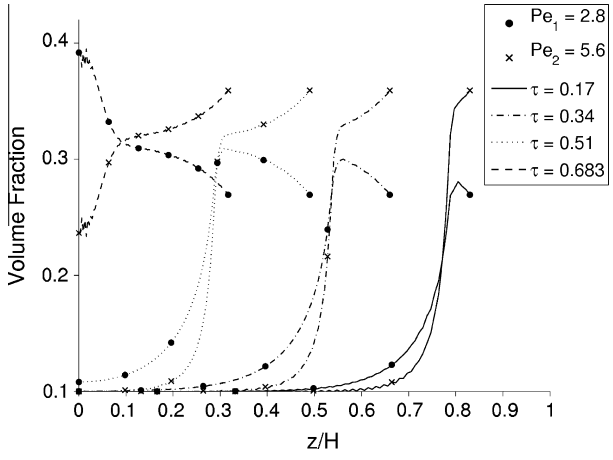

Fig. 6. Graph showing the evolution of volume fraction profiles during drying, both $Pe > 1$.

As the film dries the film/air interface moves closer to the substrate. The volume fractions of each component are represented on the vertical axes, with the profiles displayed being those of each component at various points in time during the drying process. For

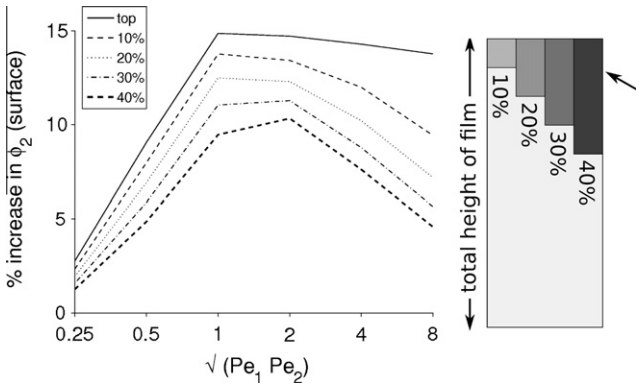

Fig. 7. Graph showing the percentage increase in component 2 through the film with varying $\sqrt{Pe_1 Pe_2}$.

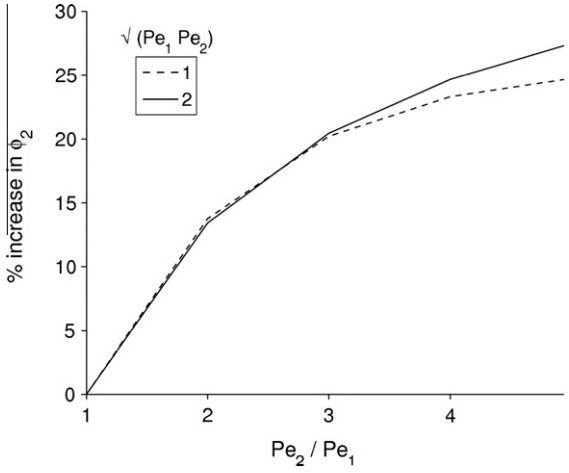

Fig. 8. Graph showing the percentage increase in component 2 in the top 10% of the film for varying Pe_2/Pe_1.

these simulations the ratio of Peclet numbers and initial volume fractions have been kept constant, with the geometric mean being the variable which has changed. Fig. 4 shows a situation where $\sqrt{Pe_1 Pe_2} \ll 1$, and as a result particles of both components diffuse quickly through the film. It can be seen that the final volume fraction profile is more uniform than subsequent graphs. Fig. 5 has a geometric mean Peclet number of unity, and as such a much greater degree of stratification is seen. When the geometric mean of the two Peclet numbers is increased, as can be seen in Fig. 6 where $\sqrt{Pe_1 Pe_2} = 4$, the middle region of the film shows less segregation, however there is still a certain degree of it close to the top and bottom of the film.

One important aspect of the analysis is how best to define and measure stratification. The basic concept revolves around comparing the final volume fraction distribution to that which would occur if the film dried completely uniformly. This can be represented as a percentage increase of a component at the surface. In all these simulations component 2 comprised the larger particles, and so it is this component which will have an increased volume fraction at the surface. Fig. 7 shows the percentage increase in component 2 from the surface, when considering an increasing percentage of the film thickness, all measured from the top surface. This is for simulations where the geometric mean Peclet number has been varied, but $Pe_1/Pe_2 = 0.5$, $\phi_1(t = 0) = 0.1$ and $\phi_2(t = 0) = 0.1$. It can clearly be seen that the trend is broadly similar regardless of how far into the film one considers. The trend is that there is enhanced stratification around $\sqrt{Pe_1 Pe_2} = 1$, as was expected based

on the dimensional analysis. Of course, when considering beyond 50% of the films' thickness there will be a considerable decrease in the stratification measured because the component with smaller particles will have a higher volume fraction in the bottom half of the film.

Because each of the curves in Fig. 7 are similar the choice of how much of the film to evaluate, to quantify the stratification, becomes arbitrary. Taking the very top surface volume fractions alone was ruled out as this did not capture the difference in stratification between $\sqrt{Pe_1 Pe_2} = 1$ and $\sqrt{Pe_1 Pe_2} = 4$ very well, yet it can be seen from Figs. 5 and 6 that there is a significant difference. However, for industrial applications it is likely that the composition close to the top surface is of the greatest interest, and so the increase in component 2 in the top 10% of the film was used as a measure of the stratification for the rest of the analysis.

Fig. 8 shows the effect of changing the ratio of the particle sizes of the two components, while keeping the initial volume fractions constant. For both $\sqrt{Pe_1 Pe_2} = 1$ and $\sqrt{Pe_1 Pe_2} = 2$ the trend is similar, with an increase in Pe_2/Pe_1 resulting in an increase in the amount of stratification observed. This can be explained due to the bigger difference between diffusion coefficients. Simulations have been run up to $Pe_2/Pe_1 = 100$, and there is in fact a maximum stratification at around $Pe_2/Pe_1 = 25$. However, long before this point the diffusion mechanics of the model become unphysical because the small particles would be able to easily flow through the voids between the larger particles. It has been suggested by Luo et al. [22] that this occurs at ratios as low as $Pe_2/Pe_1 = 6$ and a value of 7 is demonstrated by Harris et al. [25].

Figs. 9 and 10 show the evolution of volume fraction profiles when the initial concentrations of each component are varied, keeping the total initial concentration constant. A system in which there is a large starting volume fraction of larger particles can be seen in Fig. 9, whereas there is a large starting volume fraction of small particles in Fig. 10. The overall degree of stratification is shown in Fig. 11, which demonstrates that at low initial concentrations of component 2 a much higher increase in the concentration near the surface is observed. This is seen for both $\sqrt{Pe_1 Pe_2} = 1$ and $\sqrt{Pe_1 Pe_2} = 2$. While it is true that at high initial concentrations of component 2 the maximum possible percentage increase is indeed lower, this trend for much greater enrichment is still significant due to the likelihood of industrial applications being to move a small amount of an active ingredient to the surface of a coating.

The effect of changing the total particle concentration is shown in Fig. 12. As is intuitively expected a more dilute dispersion has more time to dry and therefore displays greater stratification in the final dried film. The geometric mean Peclet number that displays the maximum stratification decreases with increasing concentration because the time available for evaporation depends upon the amount of particulate material present and our scaling neglected this.

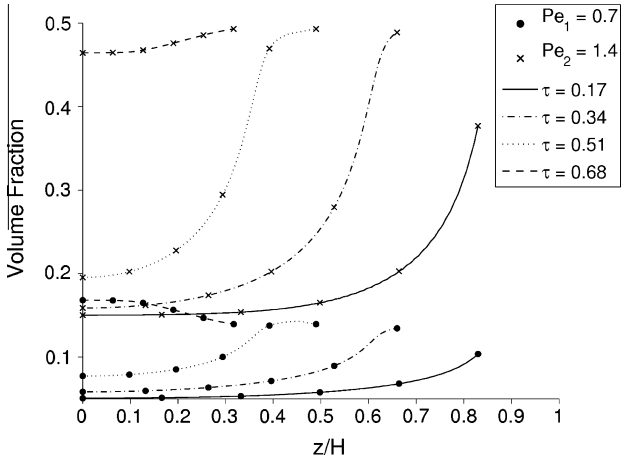

Fig. 9. Graph showing the evolution of volume fraction profiles during drying, high initial ϕ_2.

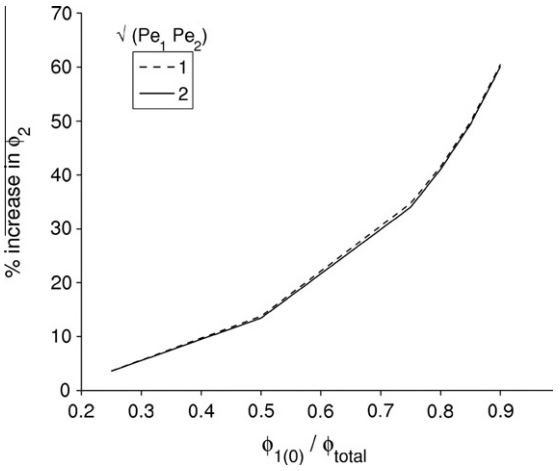

Fig. 11. Graph showing the percentage increase in component 2 in the top 10% of the film for varying $\phi_{1(0)}/\phi_{total(0)}$.

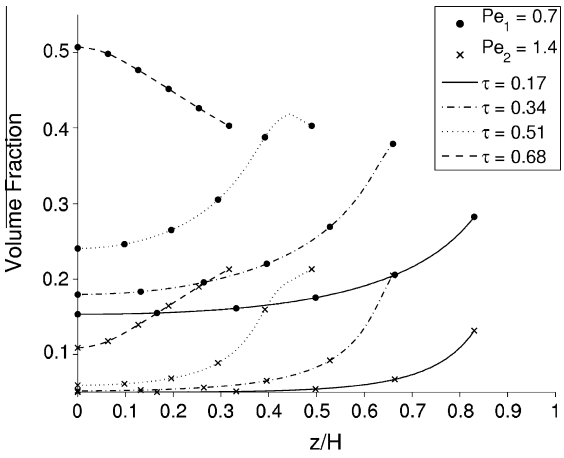

Fig. 10. Graph showing the evolution of volume fraction profiles during drying, low initial ϕ_2.

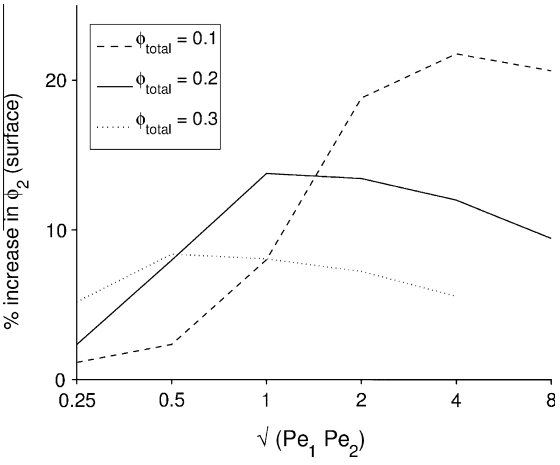

Fig. 12. Effect of changing the total initial volume fraction. In this case $Pe_2/Pe_1 = 2$ and $\phi_2(t = 0)/\phi_1(t = 0) = 1$.

Gravity is ignored in this derivation. This is usual for colloidal particles although as the particle size increases the effect of sedimentation must become increasingly important. Estimating the sedimentation velocity of particles and comparing this with the evaporation rate we conclude that for particles less than 1 μm in radius it is safe to ignore gravity. We have, in other work, (results not shown) included a gravity term and the results are qualitatively similar although with an additional accumulation of large particles towards the substrate.

This paper has derived the equations governing diffusion of bidisperse particle mixtures. These equations predict autostratification during the drying process. Experimental evidence for such a diffusional driven stratification can be found in a separate paper [26]. The techniques used are tapping mode AFM and MRI imaging.

The governing equations include the chemical potentials of the particles. This enables particle interactions to be modelled and indeed stratification can be increased by introducing a strong repulsion between particle types. The effect of particle interactions is discussed in a separate paper [27].

5. Conclusions

This paper derives the diffusion equations for particles in a two component drying film. Through numerical solution of these equations it has been demonstrated that there are a number of trends regarding the vertical stratification of two components with differing diffusion rates. The most significant of these is that the Peclet numbers must be balanced so that one component is dominated by diffusion and the other by convection so that only one is trapped by the descending film/air interface. This result displays the same trend as that seen in the work by Nikiforow et al. [20] where they saw stratification in films which were dried at rates which allowed only one component to diffuse away from the surface and not the other, but no stratification in films dried at speeds that were either too fast or too slow for this phenomena to occur.

Simulations of films with varying size ratios between particles showed that with an increase in the size ratio between the two components will lead to an increase in stratification. This is due to the increased difference in diffusion rates between the two components. It is important to note that this result is true for size ratios between 1 and 5. Above this point smaller particles within films would diffuse amongst the voids between the large particles, one example of which was demonstrated in films formed by Luo et al. [22], so simulations with larger size differences have not been reported. It has also been demonstrated that the efficiency of this stratification effect is increased with a decrease in the initial volume fraction of the larger component. This has particular importance industrially, as there are many potential advantages in being able to move a small amount of active ingredient preferentially towards the film/air interface.

There are a number of interesting avenues which could be taken to further this work, many of which are already in progress. The maximum packing fraction was taken to be 0.64 in this work, which corresponds to that of random packing of mono-disperse particles. For bi-disperse systems, the value of close-packing will vary. For example, when mixing one type of particle with another which is much larger, the small ones can fit within the voids between the larger particles, thus increasing the packing fraction. It should be trivial to add this functionality into the model, the difficulty stems from establishing the relationship between the maximum packing fraction and the relative local volume fractions of both components. The derivation method can also be expanded to a three component system, with an expression for any number of components also possible. This will be detailed in a further paper.

Experimentally there is also much that can be done, as films of two components can be dried under controlled conditions to demonstrate the behaviour described here. This paper focuses purely on the movement of the particles through diffusion controlled transport. In many systems there are many other transportation effects to consider which affect particle movement, for example convection currents, Marangoni flows and eddy recirculation [8]. Whether this size based, diffusion driven stratification can be employed in practical applications is dependent on determining whether a system can be tuned so that diffusion is a relevant particle transport process.

Acknowledgments

The authors are grateful to Prof. Diethelm Johannsmann (Clausthal University of Technology, Germany), Prof. Joe Keddie (University of Surrey), Prof. Will Zimmerman (University of Sheffield) and Dr. Stuart Clarke (University of Cambridge) for helpful discussions. R.E. Trueman was supported by a CASE award from ICI/AkzoNobel and EPSRC.

Appendix A. Supplementary material

Supplementary data associated with this article can be found, in the online version, at http://dx.doi.org/10.1016/j.jcis.2012.03.045.

References

[1] J.C. Williams, Powder Technol. 15 (2) (1976) 245–251.
[2] C.F. Harwood, Powder Technol. 16 (1) (1977) 51–57.
[3] D.L. Rowell, P.J. Dillon, Eur. J. Soil Sci. 23 (1972) 442–447.
[4] A.C. Grillet, S. Brunel, Y. Chevalier, S. Usoni, V. Ansanay-Alex, J. Allemand, Polym. Int. 53 (5) (2004) 569–575.
[5] J. Wang, J.R.G. Evans, Phys. Rev. E 73 (2) (2006). Part 1.
[6] R.D. Deegan, O. Bakajin, T.F. Dupont, G. Huber, S.R. Nagel, T.A. Witten, Nature 389 (6653) (1997) 827–829.
[7] A.F. Routh, W.B. Zimmerman, Chem. Eng. Sci. 59 (14) (2004) 2961–2968.
[8] J.L. Keddie, Mater. Sci. Eng. Rep. 21 (3) (1997) 101–170.
[9] J.L. Keddie, A.F. Routh, Fundamentals of Latex Film Formation: Processes and Properties, Springer, 2010.
[10] R.S. Krishnan, M.E. Mackay, P.M. Duxbury, C.J. Hawker, S. Asokan, M.S. Wong, R. Goyette, P. Thiyagarajan, J. Phys. Condens. Matter 19 (35) (2007).
[11] O. Vorobyova, M.A. Winnik, Macromolecules 34 (7) (2001) 2298–2314.
[12] A. DuChesne, B. Gerharz, G. Lieser, Polym. Int. 43 (2) (1997) 187–196.
[13] M.L. Jackson, B.J. Love, Polymer 45 (21) (2004) 7229–7238.
[14] J. Sun, W.W. Gerberich, L.F. Francis, Prog. Org. Coat. 59 (2007) 115–121.
[15] S.T. Eckersley, A. Rudin, Prog. Org. Coat. 23 (4) (1994) 387–402.
[16] J. Mallegol, G. Bennett, O. Dupont, P.J. McDonald, J.L. Keddie, J. Adhes. 82 (17) (2006) 217–238.
[17] A.M. Konig, T.G. Weerakkody, J.L. Keddie, D. Johannsmann, Langmuir 24 (2008) 7580–7589.
[18] E. Ciampi, P.J. McDonald, Macromolecules 36 (22) (2003) 8398–8405.
[19] P. Ekanayake, P.J. McDonald, J.L. Keddie, Eur. Phys. J. – Special Top. 166 (2009) 21–27.
[20] I. Nikiforow, J. Adams, A.M. Konig, A. Langhoff, K. Pohl, A. Turshatov, D. Johannsmann, Langmuir 26 (16) (2010) 13162–13167.
[21] H. Luo, L.E. Scriven, L.F. Francis, JCIS 316 (2007) 500–509.
[22] H. Luo, C.M. Cardinal, L.E. Scriven, L.F. Francis, Langmuir 24 (10) (2008) 5552–5561.
[23] F. Buss, C.C. Roberts, K.S. Crawford, K. Peters, L.F. Francis, JCIS 359 (2011) 112–120.
[24] D.J. Harris, H. Hu, J.C. Conrad, J.A. Lewis, Phys. Rev. Lett. 98 (148) (2007) 301–304.
[25] D.J. Harris, H. Hu, J.C. Conrad, J.A. Lewis, Philos. Trans. R. Soc. A 367 (1-2) (2009) 5157–5165.
[26] R.E. Trueman, E. Lago Domingues, S.N. Emmett, M.W. Murray, J.L. Keddie, A.F. Routh, Langmuir (2012), http://dx.doi.org/10.1021/la203975b.
[27] A. Atmuri, S.R. Bhatia, A.F. Routh, Langmuir 28 (5) (2012) 2652–2658.
[28] C.F. Curtiss, R.B. Bird, Ind. Eng. Chem. Res. 38 (1999) 2515–2522.
[29] E.L. Cussler, Diffusion: Mass Transfer in Fluid Systems, Cambridge University Press, 1984. pp. 194–211.
[30] J.L. Lebowitz, J.S. Rowlinson, J. Chem. Phys. 41 (1964) 133–138.
[31] W.B. Russel, D.A. Saville, W.R. Schowalter, Colloidal Dispersions, Cambridge University Press, 1991.